DOI: 10.1038/ncb3225

nature cell biology

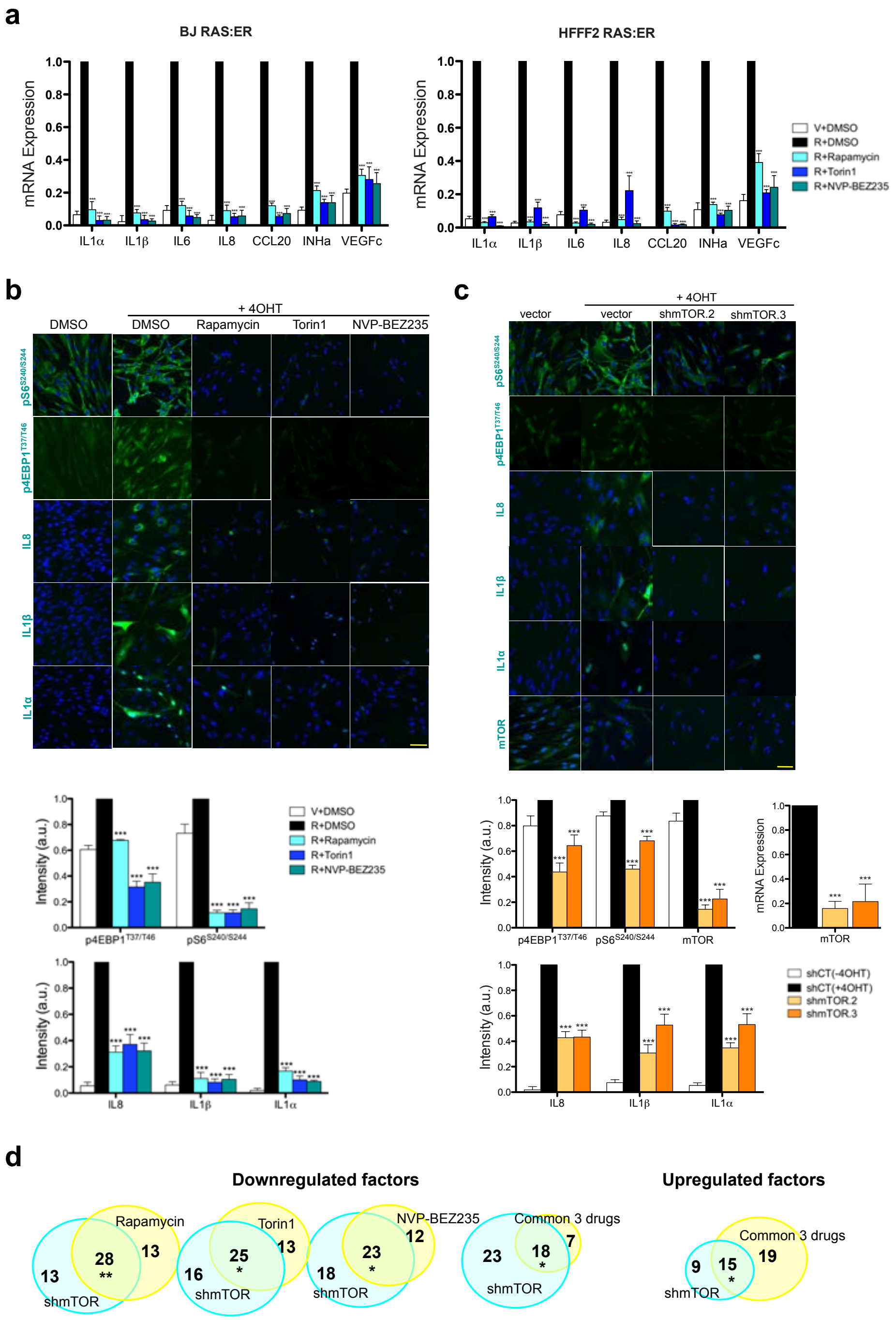


**Supplementary Figure 1** mTOR inhibition regulates the SASP. **a.** mTOR inhibition regulates the SASP in different fibroblasts strains. BJ ER:RAS and HFFF2 ER:RAS cells were generated and induced with 4OHT to activate ER:RAS in the presence of 10 nM rapamycin, 25 nM Torin1 or 0.5 nM NVP-BEZ235. Seven days after 4OHT induction, RNA was collected and qPCRs performed to detect the expression of selected SASP components. Data are mean ± s.d. from *n*=3 independent experiments. Student's T-test was performed to compare the different treatments to the control (R+DMSO) with *** P < 0.001. V, cells expressing an empty vector; R, cells infected with pLNC-ER:RAS .**b, c.** mTOR inhibition (b) or mTOR knockdown (c) decreases phosphorylation of S6 (pS6$^{S240/S244}$) and eIF4EBP1 (p4EBP1$^{T37/T46}$) proteins and inhibits the induction of the SASP. Indicated immunostainings were performed 7 days after 4OHT induction. Fold changes of normalised values and representative images are shown. Error bars represent the ± s.d. from *n*=4 independent experiments. Student's T-test was performed to compare treated/shMTOR cells to the control senescent cells. *** P < 0.001. Scale bar, 30 μm. **d.** Venn diagrams representing the overlap and significance for the SASP components downregulated or upregulated by multiple mTOR inhibitors and mTOR knockdown. The significance of overlap was computed using hypergeometric test. ** P < 0.01; *P < 0.05. For raw data, see Supplementary Table 7.



© 2015 Macmillan Publishers Limited. All rights reserved

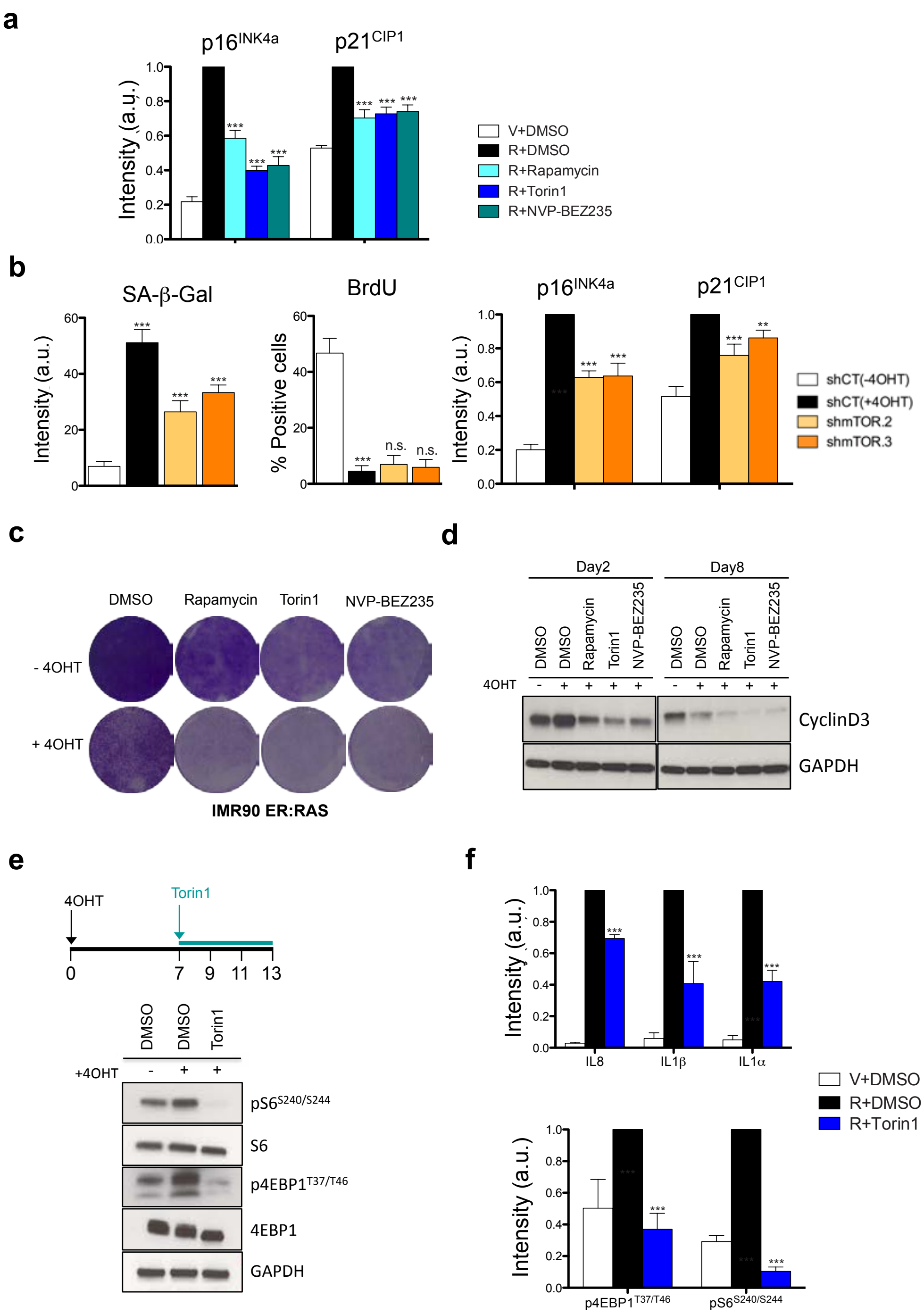


**Supplementary Figure 2** mTOR inhibition controls the senescence phenotype and cell proliferation. **a.** mTOR inhibition decreases the levels of cell cycle inhibitors involved in senescence. $p16^{INK4a}$ and $p21^{CIP1}$ levels were measured in the same experimental settings as in Supplementary Fig. 1b. Error bars represent the ± s.d. from *n*=3 independent experiments. **b.** mTOR knockdown results in decreased SA-β-Gal activity, $p16^{INK4a}$ and $p21^{CIP1}$ levels but cells remain arrested. BrdU incorporation and senescence markers were determined after 7 days of induction with 4OHT. Data are mean ± s.d. from *n*=6 (BrdU) and *n*=4 (SA-β-Gal, p16 and p21) independent experiments. Student's T-test was performed to compare the shmTOR cells with the senescent controls (shCT+4OHT). *** $P < 0.001$; ** $P < 0.01$: n.s, non significant. **c.** mTOR inhibition decreases proliferation of normal IMR90 human fibroblasts and does not rescue OIS arrest. IMR90 ER:RAS cells ($2 \times 10^4$) were treated as indicated and proliferation was assessed by CV staining after 14 days in culture. Images are representative of 3 independent experiments. **d.** Cyclin D3 expression levels were assessed by immunoblot. IMR90 ER:RAS cells were left untreated or treated with 4OHT and the indicated drugs for 2 or 8 days. Data are representative of *n*=3 independent experiments. **e-f.** These figures are an extension of the experiment presented in Fig. 2b-c**.** Torin1 inhibition of mTOR downstream targets ($pS6^{S240/S244}$, $p4EBP1^{T37/T46}$) and the SASP was assessed by immunoblot (e) and IF (f) 7 days after 4OHT induction. Immunoblots are representative of *n*=3 independent experiments. Error bars represent the ± s.d. from *n*=4 independent experiments. Student's T-test was performed to compare Torin1 treated cells to the control. *** $P < 0.001$. Unprocessed original scans of blots are shown in Supplementary Fig. 9. For raw data, see Supplementary Table 7.



© 2015 Macmillan Publishers Limited. All rights reserved

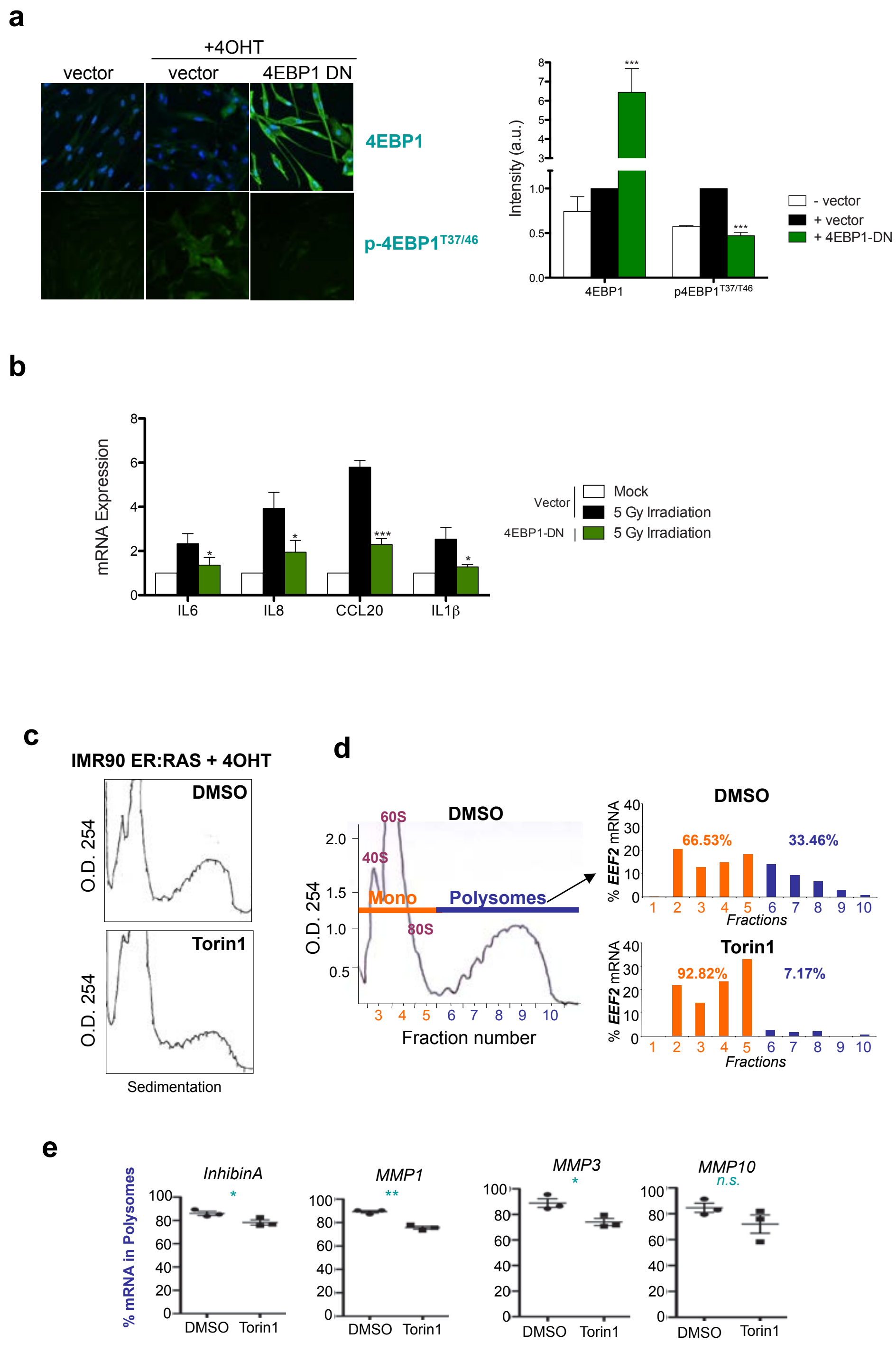


**Supplementary Figure 3** Effect of mTOR and 4EBP1 on the translation of SASP components. **a.** This is an extension of Figure 3a-c. Expression of an eIF4EBP1 phospho-mutant (4EBP1 DN) results in decreased phosphorylated 4EBP1$^{Thr37/46}$ levels. (right) Fold changes of normalised intensity values obtained from 4EBP1 and 4EBP1$^{Thr37/46}$ immunostainings Data are mean ± s.d. from *n*=3 independent experiments**.** (left) Images from a representative experiment are shown. Data are mean ± s.d. from *n*=3 independent experiments**.** For all graphs, student's T-test was performed to compare cells expressing a 4EBP1 DN to the control (+ vector). *** P < 0.001. Scale bar, 30 μm. **b.** Expression of 4EBP1 DN impairs the SASP levels observed in irradiated IMR90 fibroblasts. RNA was collected 8 days after irradiation (5 Gy). Data are mean ± s.d. from *n*=3 independent experiments. Student's T-test was performed to compare the cells expressing 4EBP1-DN to the control (vector irradiated). *** P < 0.001; *P < 0.05 **c.** Profile of mTOR-regulated translation in OIS. Representative polysome profiles of IMR90 ER:RAS cells (incubated for 6 days with 4OHT) treated with DMSO or 250 nM Torin1 for 3 h from *n*=3 independent experiments. **d.** A schematic representation of the position of fractions (3–10), monosomes and polysomes is shown together with a representative profile for EEF2 mRNA (a canonical mTOR target). Data are representative of 3 independent experiments. **e** Polysome analysis of mRNAs for SASP components. Graphs show the percentage of the indicated mRNAs in actively translating polysomes during OIS. Error bars represent the ± s.d. from *n*=3 independent experiments. Student's T-test was performed to compare Torin1 treated cells to the DMSO-treated controls. *** P < 0.001; ** P < 0.01; *P < 0.05; N.S, non significant. For raw data, see Supplementary Table 7.



© 2015 Macmillan Publishers Limited. All rights reserved

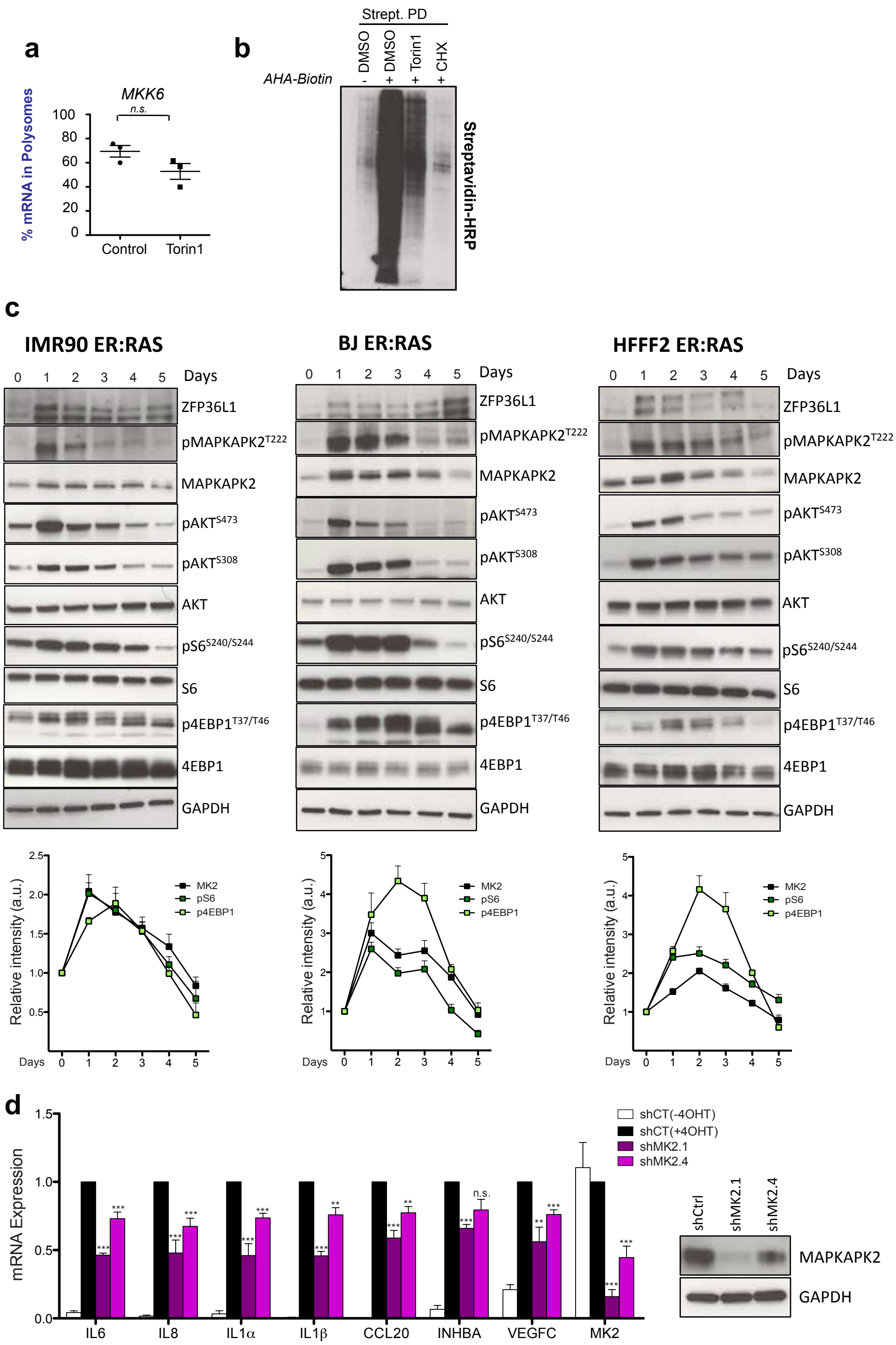


**Supplementary Figure 4** MAPKAKP2 regulates the SASP. **a.** Polysome distribution of MKK6 mRNA. Error bars represent the ± s.d. from *n*=3 independent experiments. Student's T-test was performed to compare Torin1 treated cells to the control. n.s., non significant. **b.** Related to Fig 4e. Samples were immunoblotted with Streptavidin-HRP to detect AHA-Biotin containing proteins. Samples purified by pull down with streptavidin beads (Strept. PD) were analysed. Data are representative of 3 independent experiments. **c.** MAPKAPK2 protein levels correlate with mTOR signalling. IMR90 ER:RAS, BJ ER:RAS and HFFF2 ER:RAS cells were left untreated or treated with 4OHT for the indicated times. (Top) Immunoblots were performed with the indicated antibodies. Data are representative of 3 independent experiments. (Bottom) Quantification of MK2, $pS6^{S240/S244}$ and $p4EBP1^{T37/T46}$ blots. Error bars represent the ± s.d. from *n*=3 independent experiments. **d.** MAPKAPK2 inhibition prevents SASP induction. IMR90 ER:RAS cells were infected with the indicated hairpins and further treated with 4OHT. RNA and protein extracts were collected at day 6 after induction. Expression of the SASP and MK2 were assessed by qRT-PCR (left) or immunoblotting (right). Immunoblot images are representative of 3 independent experiments. Error bars represent the ± s.d. from *n*=3 independent experiments. Student's T-test was performed to compare cells deficient for MK2 to control cells (shCT + 4OHT ). *** $P < 0.001$; ** $P < 0.01$; *$P < 0.05$; N.S, non significant. Unprocessed original scans of blots are shown in Supplementary Fig. 9. For raw data, see Supplementary Table 7.



© 2015 Macmillan Publishers Limited. All rights reserved

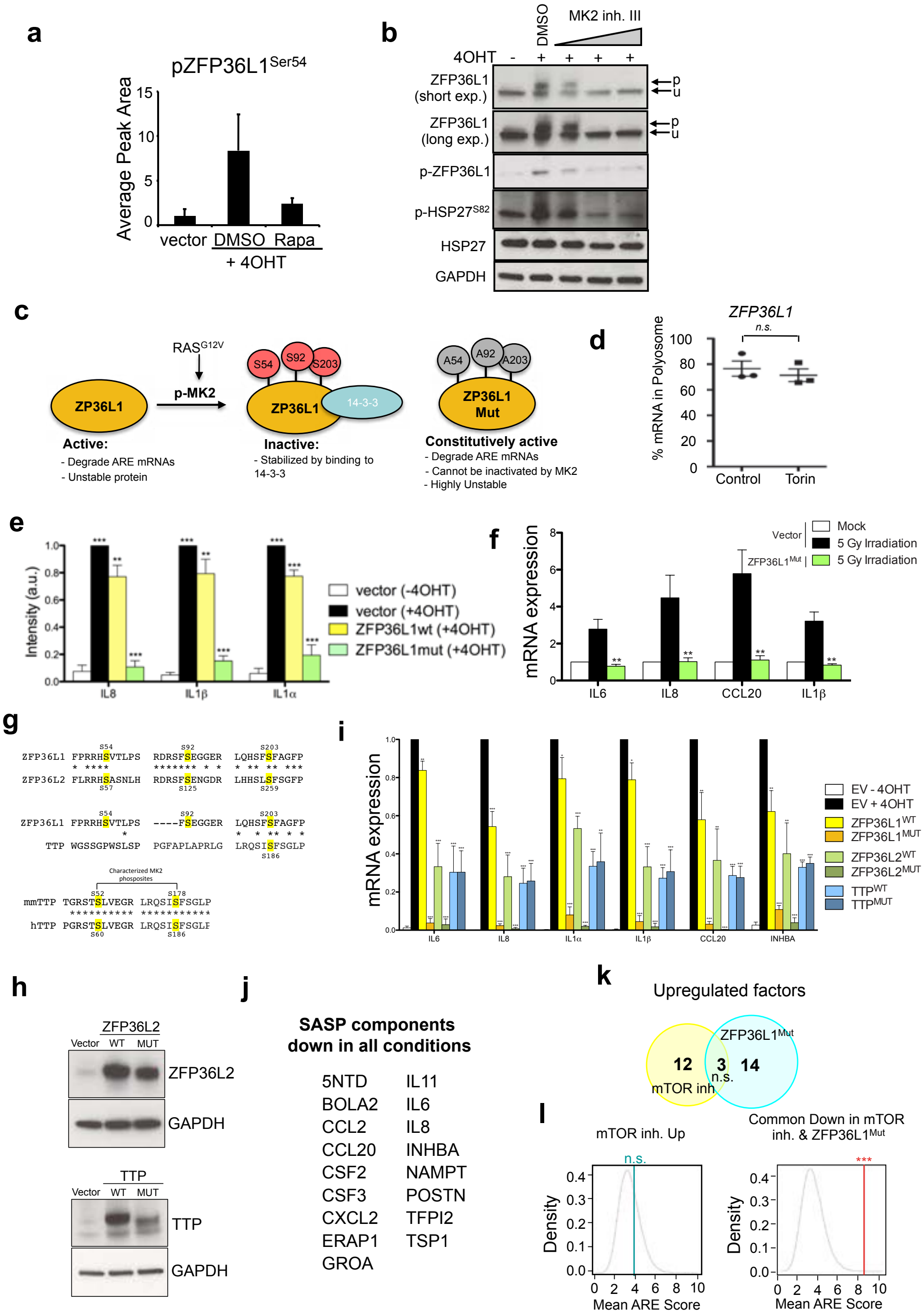


**Supplementary Figure 5** ZFP36L1 regulates the SASP. **a.** Serine54 in ZFP36L1 was identified as an mTOR inhibition-sensitive phosphosite by phosphoproteomics (*n*=3). **b.** Extension of Fig 5b. Specificity of MK2 inhibitor III is proved by the decrease in the phosphorylation of HSP27 (pHSP27$^{S82}$) a downstream target of MK2. **c.** Schematic model of ZFP36L1 activity and protein stability. **d.** Percentage of ZFP36L1 mRNA in translating polysomes during OIS (*n*=3) **e.** IMR90 ER:RAS cells were infected as indicated. Immunostainings were performed 7 days after 4OHT induction. Fold changes of normalised intensity values are shown (*n*=4). **f.** SASP genes expression was measured in IMR90 fibroblasts 8 days after irradiation (5 Gy) (*n*=3). **g.** Designed TTP and ZFP36L2 phosphomutants. Since MK2 phosphosites for TTP and ZFP36L2 have not been described, we aligned their sequences with that of ZFP36L1 aiming to identify putative MK2 phosphosites. In the case of TTP, homology is low. However, the two known MK2 phosphosites in the murine form of TTP[59] are conserved in the human form. **h-i.** IMR90 ER:RAS cells were infected with ZFP36L1$^{wt/mut}$, ZFP36L2$^{wt/mut}$ or TTP$^{wt/mut}$. OIS was induced by 4OHT for 7 days. **(h)** Protein levels were analysed by immunoblot in presence of MG132 (2 μM, 12h). **(i)** Expression of SASP genes was measured by qRT-PCR (*n*=3). **j.** SASP components detected in our proteomics analysis that are downregulated by mTORinhibitors, shmTOR and ZFP36L1$^{Mut}$. **k.** Venn diagrams representing the overlap between SASP factors upregulated by mTOR inhibitors, shmTOR and ZFP36L1$^{Mut}$. **l.** ARE Score for SASP factors: (left) commonly upregulated by shmTOR and mTOR inhibitors; (right) commonly downregulated by shmTOR, mTOR inhibitors and ZFP36L1$^{Mut}$. Plots denote ARE score distribution for $10^5$ random combinations of 15 and 17 mRNAs respectively. Statistical significance was calculated by using: (**d,e,j and i:** Student's *t*-test) (**k:** hypergeometric test), (**l:** permutation tests). *** P < 0.001; ** P < 0.01; *P < 0.05; n.s, non significant. Error bars represent means ± s.d. For **b** and **h** data are representative of 3 independent experiments. *n* represents number of independent experiments. For unprocessed original scans of blots, see Supplementary Fig. 9. For raw data, see Supplementary Table 7.



© 2015 Macmillan Publishers Limited. All rights reserved

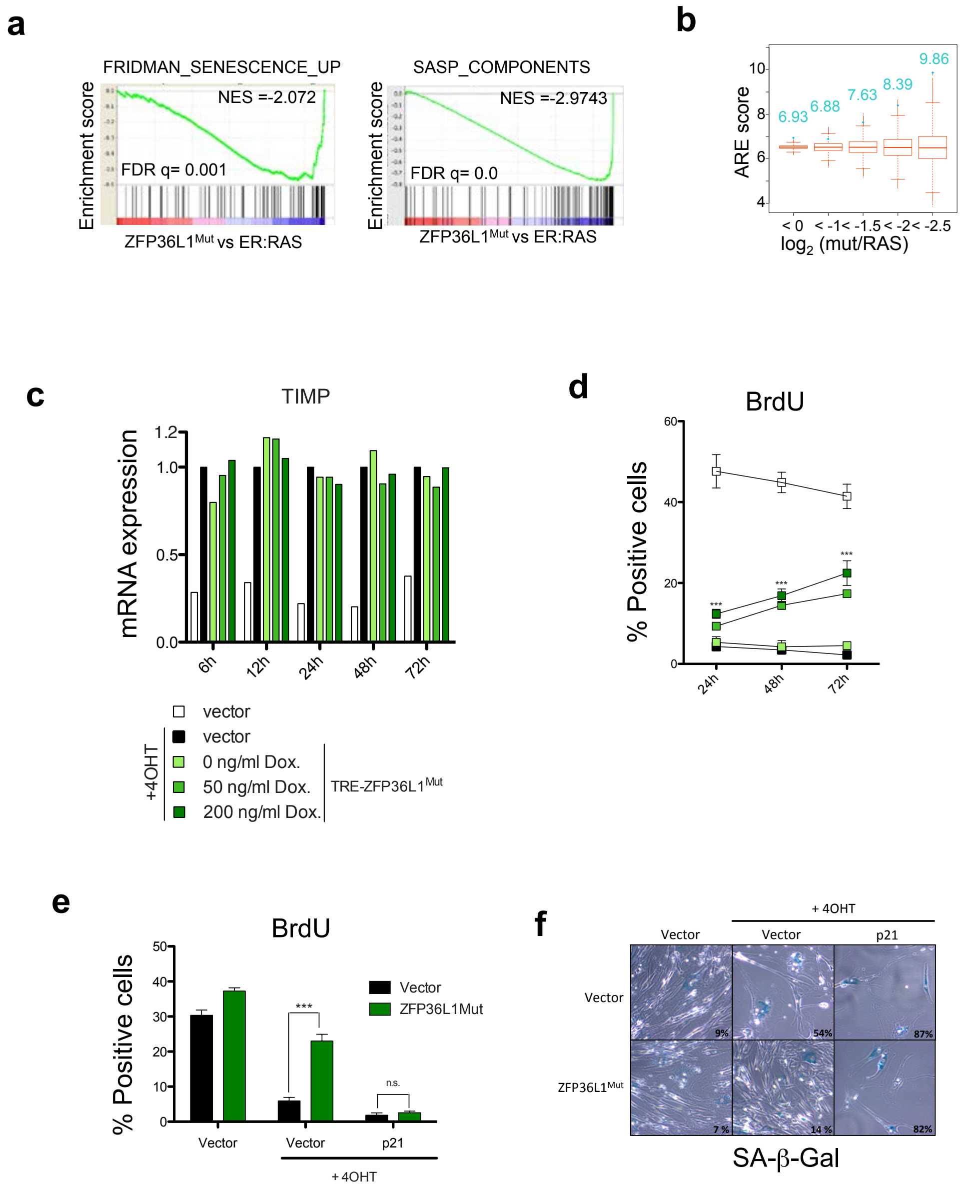


**Supplementary Figure 6** Further characterization of the role of ZFP36L1 in the regulation of the SASP. **a.** GSEAs of a signature associated with senescenc [60] and (left) SASP components upregulated in OIS [6] (right) in the gene expression profile (GEP) of IMR90 ER:RAS cells expressing ZFP36L1$^{Mut}$ versus control IMR90 ER:RAS, both 4OHT-treated. NES, normalized enrichment score; FDR, false discovery rate. GEPs were obtained by performing transcriptome sequencing (RNA-Seq) of the aforementioned conditions in $n$=3 independent experiments. RNAs were collected 7 days after induction with 4OHT. **b.** Mean ARE score of genes down regulated (at the indicated $\log_2$ of fold changes) when comparing IMR90 ER:RAS cells expressing ZFP36L1$^{Mut}$ versus control IMR90 ER:RAS, are shown in blue. The distribution of mean ARE scores derived from $10^5$ simulations of random genes with equal sample size are shown in red. **c.** This is an extension of Figure 6c. The expression of TIMP was monitored by qRT-PCR at the indicated times. Data are for a representative experiment of $n$=2 independent experiments. **d** Brdu incorporation was measured by IF at the indicated times. Error bars represent the ± s.d. from $n$=3 independent experiments. Student's T-test was performed to compare ZFP36L1$^{Mut}$ expressing cells (200ng/ml doxycycline) to the control senescent cells (vector, +4OHT). *** P < 0.001.**e-f.** IMR90 ER:RAS expressing TRE-FLAG-ZFP36L1$^{Mut}$ (or empty vector) and the reverse transactivator (rtTA-M3) were further infected with a vector encoding the coding sequence of p21. After 6 days of incubation with 4OHT, the expression of ZFP36L1$^{Mut}$ was induced with 200ng/ml doxycycline for 72h and (e) the % of BrdU positive cells or (f) SA-β-Gal positive cells was quantified. Error bars represent the ± s.d. from $n$=4 independent experiments. SA-β-Gal stainings are representative of $n$=3 independent experiments. Student's T-test was performed to compare the indicated conditions ***P< 0.001; n.s., non significant. For raw data, see Supplementary Table 7.



© 2015 Macmillan Publishers Limited. All rights reserved

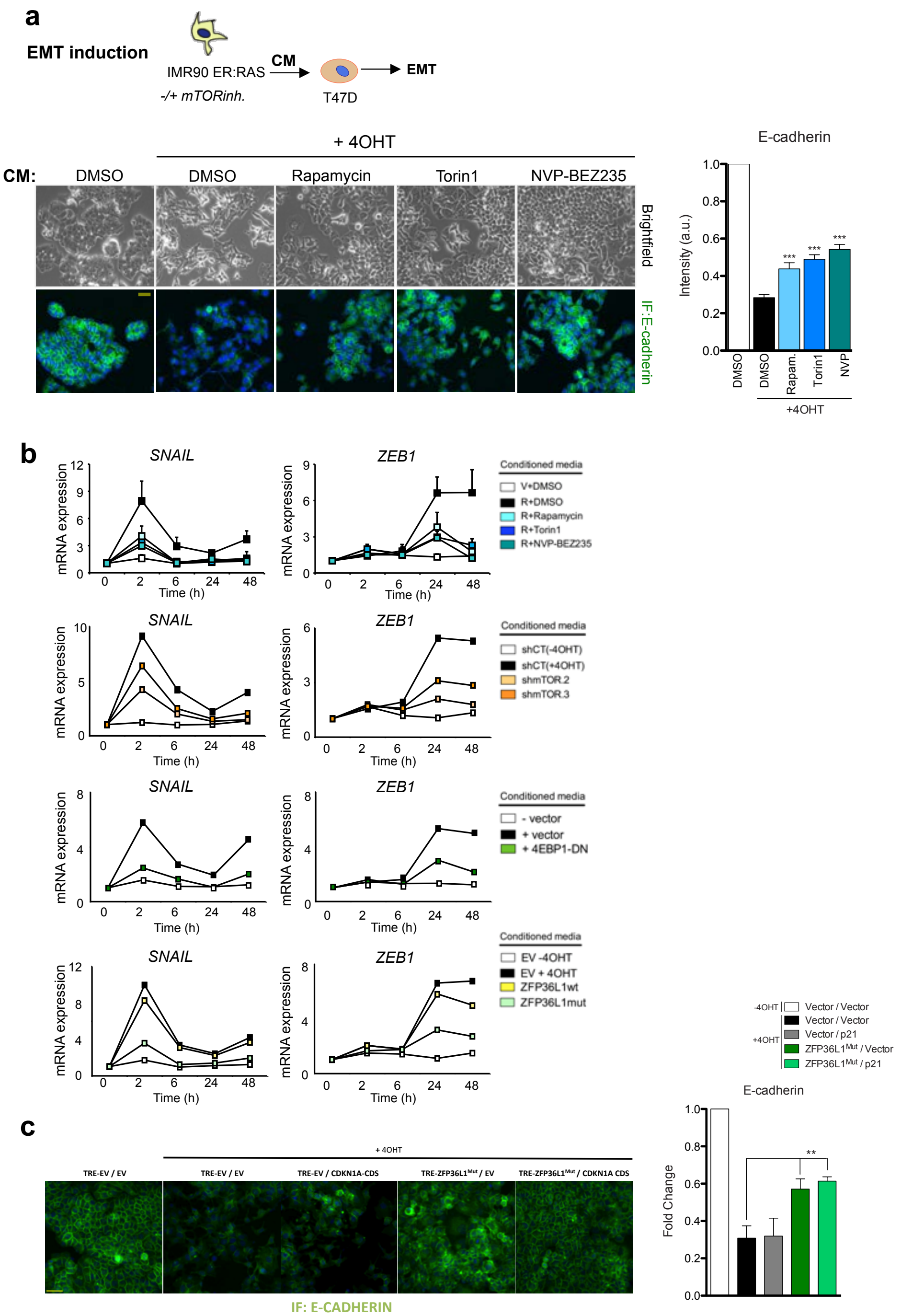


**Supplementary Figure 7** The paracrine protumorigenic effects of senescent cells are sensitive to mTOR inhibition and ZFP36L1 activity. **a.** mTOR inhibition prevents the EMT induced by the CM of senescent cells. IMR90 ER:RAS cells were treated as indicated in the scheme. CM was collected 7 days after 4OHT induction (mTOR inhibitors were removed from the media at day 4, *see methods for details*) and T47D cells cultured in that CM. 48h after, E-Cadherin expression was monitored by IF. Fold changes of normalised intensity values (top) and representative pictures are shown (bottom). Data are mean ± s.d. from *n*=4 independent experiments. Student's T-test was performed to compare treated cells to the control. *** P < 0.001. Scale bar, 40μm. **b.** Both inhibition of mTOR signalling and expression of ZFP36L1$^{Mut}$ prevent the upregulation of EMT-specific transcription factors by the CM of senescent cells. IMR90 ER:RAS cells were treated as indicated in the scheme in (a). CM was collected after 7 days. T47D cells were cultured in that CM for the indicated times and processed for RNA extraction. Snail1 and Zeb1 mRNA expression levels were measured by qRT-PCR. In the case of the CM of IMR90 ER:RAS treated with mTOR inhibitors, data are mean ± s.d. from *n*=3 independent experiments. For the rest of the experiments data are from a representative experiment of *n*=2 independent experiments. **c.** CM of both proliferating and arrested ZFP36L1$^{Mut}$ expressing cells is unable to trigger a complete EMT. The indicated cells were treated with 4OHT for 9 days. Expression of TRE-ZFP36L1$^{Mut}$ was activated for the last 72h. CM was then collected and T47D cells were cultured in that CM for 48h. E-Cadherin expression was monitored by IF. Fold changes of normalised intensity values (right) and representative pictures are shown (left). Data are mean ± s.d. from *n*=3 independent experiments.. Student's T-test was performed to compare ZFP36L1$^{Mut}$ cells to the control (Vector/ Vector). ** P < 0.01. Scale bar, 40μm. For raw data, see Supplementary Table 7.



© 2015 Macmillan Publishers Limited. All rights reserved

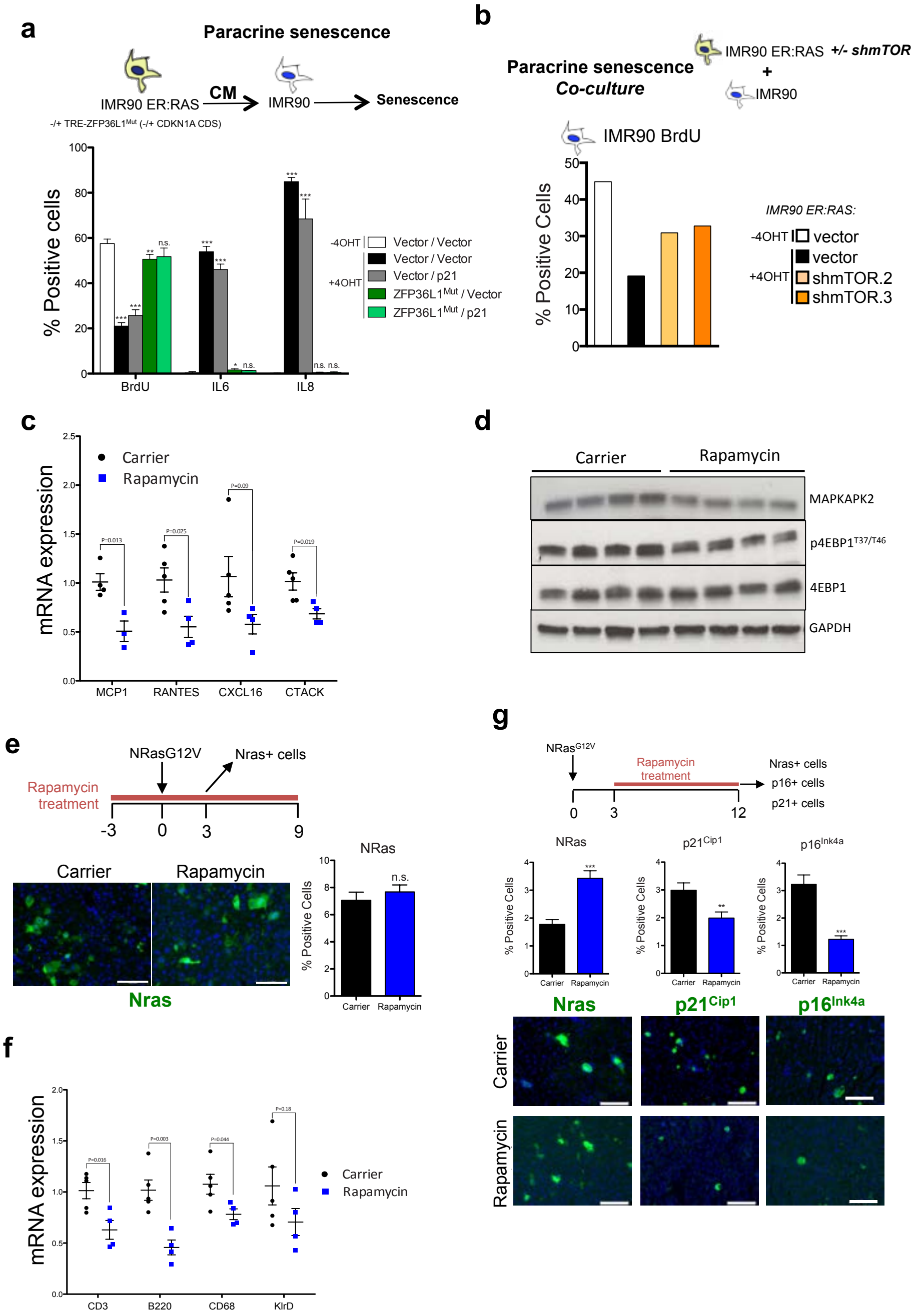


**Supplementary Figure 8** mTOR inhibition blunts the tumour suppressive effects of the SASP. **a.** CMs of IMR90 ER:RAS expressing TRE- ZFP36L1$^{Mut}$ (or empty vector) and p21 (or empty vector) were collected 72h after induction of ZFP36L1$^{Mut}$ and 9 days after 4OHT addition. The effect CMs had on BrdU incorporation and SASP induction in IMR90 wt cells was evaluated by IF. Graphs show data from *n*=4 independent experiments **b.** IMR90 wt cells were co-cultured with the indicated IMR90 ER:RAS cells with or without 4OHT. BrdU incorporation was monitored by IF. Data are representative of *n*=2 independent experiments. **c.** This figure is related to Fig. 8c. Expression of the indicated transcripts was quantified by qRT-PCR. Carrier, *n*=5 mice; Rapamycin, *n*=4 mice. P values are included. **d.** Expression of MAPKAPK2, 4EBP1 and phosphorylation of 4EBP1 were analysed by immunoblot. Quantification is presented in Fig 8d. **e.** Nras$^{G12V}$ transposons were co-delivered into mouse livers through hydrodynamic injection (Day 0). Mice were sacrificed 3 days later and Nras+ cells were counted (*n*=4 mice per condition) Mice were treated with carrier or drugs from 3 days prior Nras$^{G12V}$ injection. Representative images of the sections quantified are shown (200x). Scale bar, 100μm. **f.** Quantification of the expression of immune cell markers by qRT-PCR in livers of the indicated mice 6 days after NrasG12V injection. Carrier, *n*=5 mice; rapamycin, *n* =4 mice. CD3, T cell marker; B220, B cell marker; CD68, macrophage marker; KlrD, NK cell marker. P values are included. **g.** Nras$^{G12V}$ transposons were co-delivered into mice as explained before. Mice were sacrificed 12 days later. Mice were only treated with carrier or rapamycin 3 days post-injection Nras+ (left), p21$^{Cip1}$+ (centre) and p16$^{Ink4a}$+ (right) cells on liver sections were counted (*n*=4 mice per condition). Representative images of sections quantified in the top panel are shown in the bottom. Scale bar, 100μm. Statistical significance was calculated using Student's *t*-test, *** P < 0.001; ** P < 0.01; * P < 0.05; n.s, non significant. Error bars represent means ± s.d. For unprocessed original scans of blots, see Supplementary Fig. 9. For raw data, see Supplementary Table 7.



© 2015 Macmillan Publishers Limited. All rights reserved

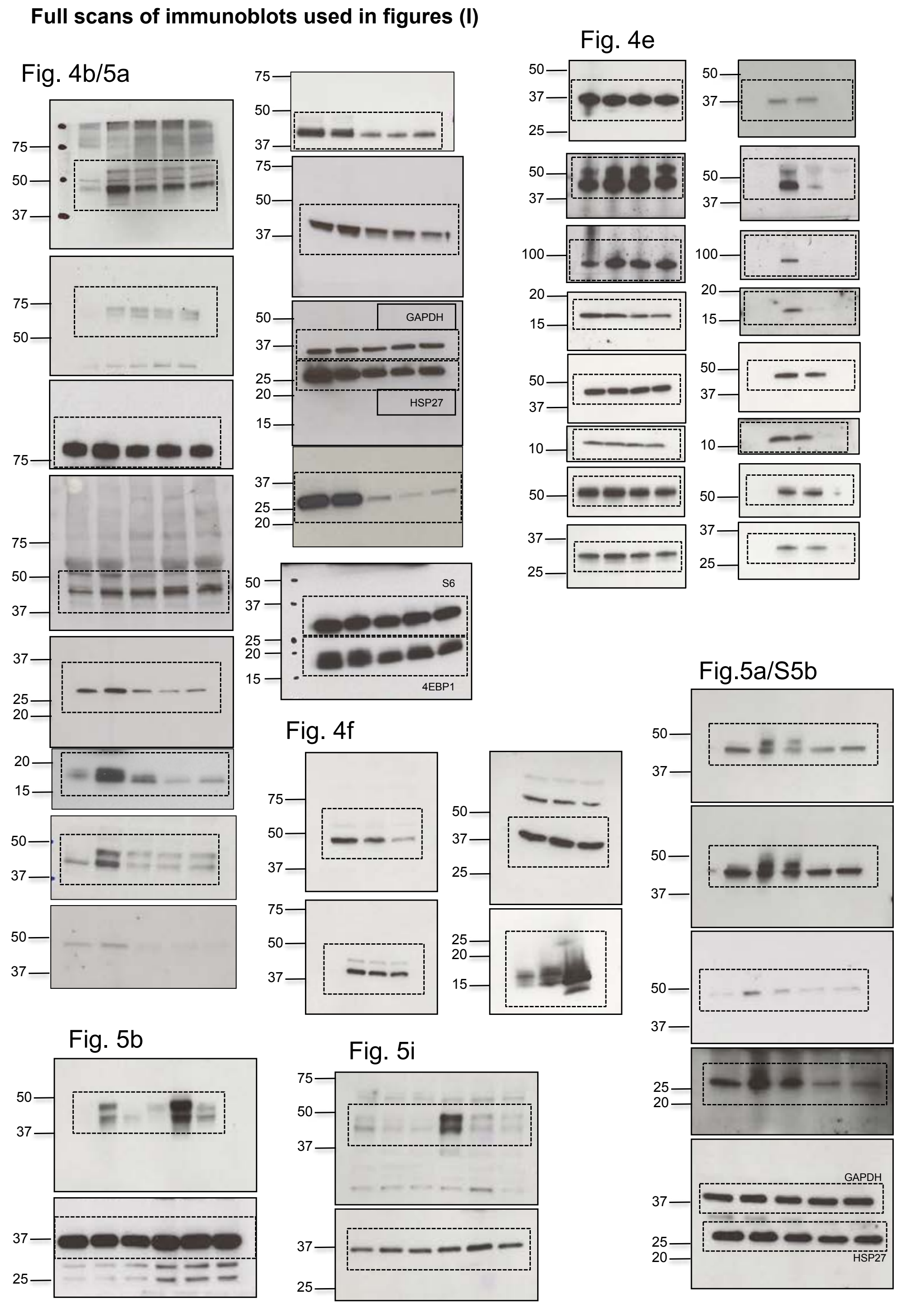


**Supplementary Figure 9** Full scans of immunoblots used in figures.



© 2015 Macmillan Publishers Limited. All rights reserved

**Full scans of immunoblots used in figures (II)**

Fig. 6b

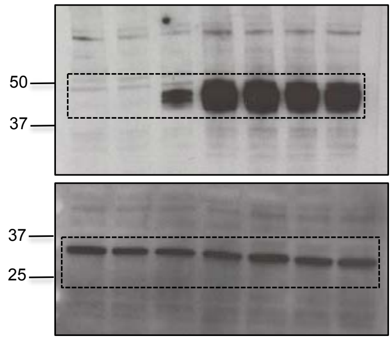

Fig. S2d

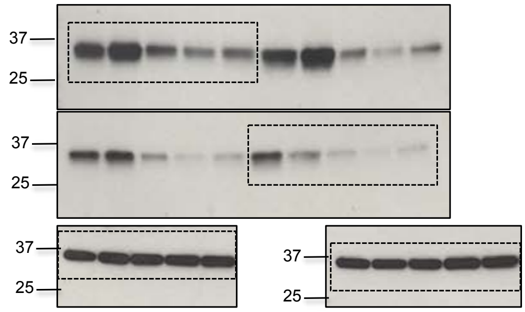

Fig. S2e

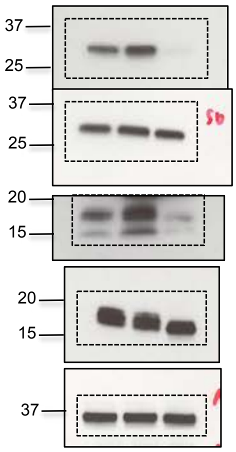

Fig. S4c (IMR90)

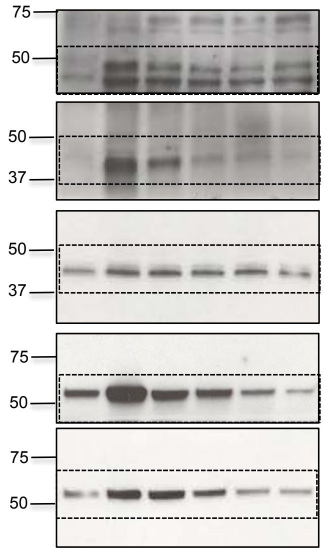

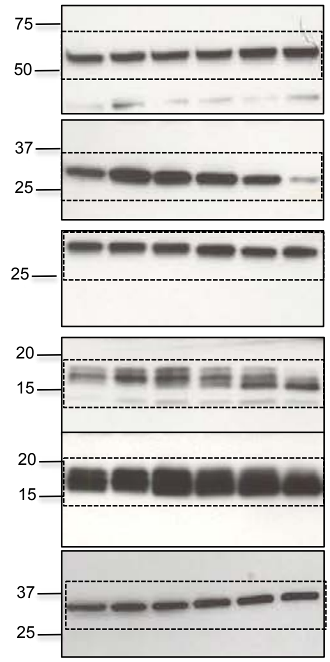

Fig. S4c (BJ)

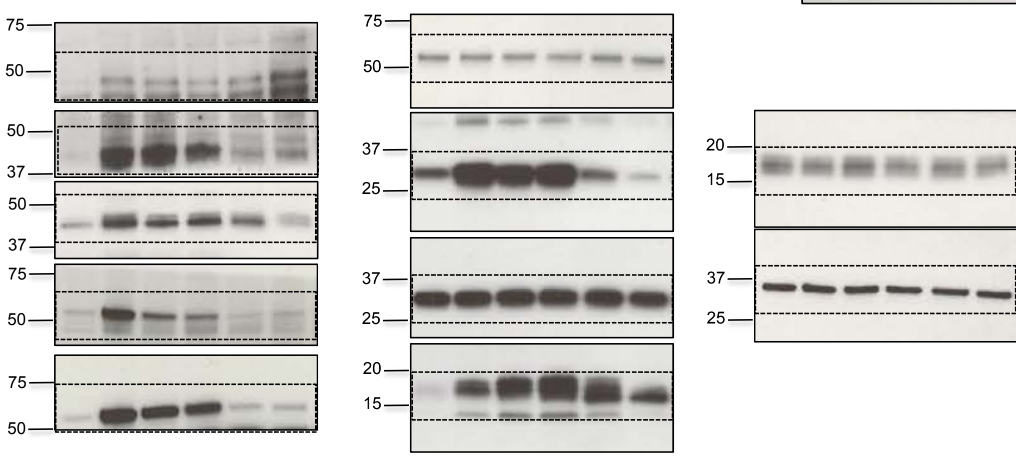

**Supplementary Figure 9 continued**



© 2015 Macmillan Publishers Limited. All rights reserved

## Full scans of immunoblots used in figures (III)

Fig. S4c (HFFF2)

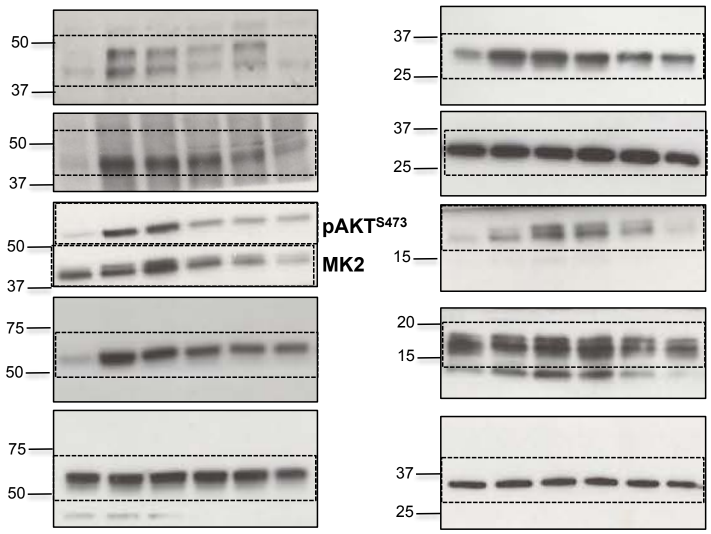


Fig. S4d

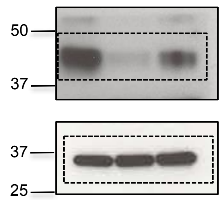


Fig. 6d

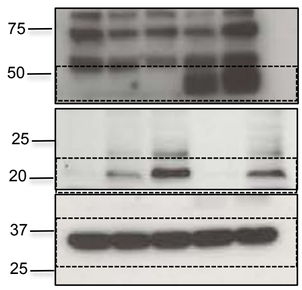


Fig. 8e

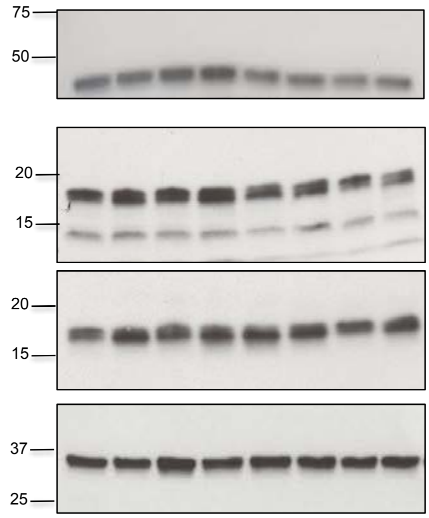


Fig. S6g

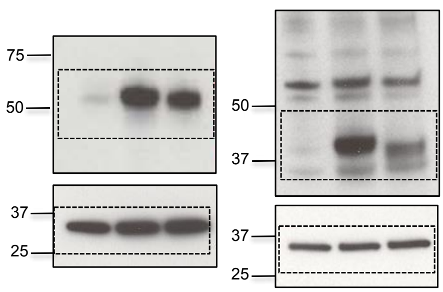


Supplementary Figure 9 continued



© 2015 Macmillan Publishers Limited. All rights reserved

**Supplementary Tables Legends**

**Table S1** Effect of the chemical compounds in the mRNA expression levels of key SASP components.
**Table S2** Secretome proteomics data for mTOR inhibitors (normalised values).
**Table S3** Phosphoproteomic data.
**Table S4** Chemical compounds used in the drug screen.
**Table S5** Primers, Taqman probes and RNAi sequences used in this study.
**Table S6** Antibodies used in this study.
**Table S7** Raw data.



© 2015 Macmillan Publishers Limited. All rights reserved